PACS numbers: 07.60.–j; 42.15.Dp; 42.79.Kr
DOI: 10.1070/QE2002v032n04ABEH002199

Electrophysics of a modal multichannel liquid-crystal wavefront corrector

I.P.Guralnik, S.A.Samagin

***Abstract*. The impedance of a modal multichannel wavefront corrector is studied theoretically and experimentally for the first time. The theoretical model takes into account the dependence of liquid crystal parameters on the control voltage frequency. These dependences were measured separately. It is found that the equivalent capacitance and resistance of the corrector in the frequency region up to 1 kHz are determined by the ionic conductivity of the liquid crystal, whereas at higher frequencies the frequency dependence of the local voltage comes into play. The theoretical results well agree with the experimental data.**

Keywords: *wavefront correctors, liquid crystals, electric impedance.*

1. Introduction

Liquid crystal (LC) phase modulators are an attractive alternative to deformable mirrors for applications in low-cost adaptive optics systems. Along with a usual LC cell, which is employed as the zero-order wavefront corrector, LC prisms, spherical [1] and cylindrical [2] lenses are also being used. The latter devices belong to the so-called modal wavefront correctors [3]. Aside from lenses, multichannel LC correctors have been developed [4, 5], which provide a more precise control of the radiation wavefront. A multichannel LC corrector (MLCC) uses in fact both the modal and zonal control. Because the modal control is based on variation of the amplitude and frequency of the control voltage, a 37-channel corrector has 74 degrees of freedom.

In the above-mentioned papers, the general principles of the operation of MLCCs were considered and the results of calculations of the axially symmetric distribution of the control voltage over its aperture and of measurements of its amplitude and phase were reported. The charge transfer in the MLCC and the equivalent electric parameters describing the MLCC as a two-terminal network were not analysed. However, it is known [6, 7] that the dynamic capacitance and resistance of LC devices also give valuable information on their electrooptical properties because the reorientation of LC molecules in an electric field (the Fredericksz transition) is accompanied by a change in their optical and dielectric properties. On the other hand, the absolute values of the capacitance and resistance of the MLCC determine the type of a load that the MLCC represents for input cascades of the control-unit channels and, therefore, the analysis of these parameters is important for the development of the control unit and its coupling with the MLCC.

In this paper, we studied theoretically and experimentally the equivalent electric parameters of the MLCC in the operating frequency region. We calculated for the first time the MLCC impedance and measured its equivalent capacitance and resistance. To perform a correct comparison of the theoretical calculations with experimental data, we also studied the complex permittivity of the LC in the corresponding frequency region.

2. Calculation of the MLCC impedance

Fig. 1 shows the MLCC design. An LC layer is sandwiched between two glass substrates with alignment coatings (not shown in Fig. 1) and conducting layers deposited on them. One of the layers has low resistance, so that the potential at all its points is the same. Another electrode, the so-called control electrode, has high resistance of about 1 MΩ/□. It is deposited on a glass substrate to which thin metal contacts are implanted. If an ac voltage is applied to the contacts relative to the low-resistance electrode, then because of the modal effect [1] the voltage at the control electrode will be distributed according to a certain law, which depends on the frequency of the applied voltage. As

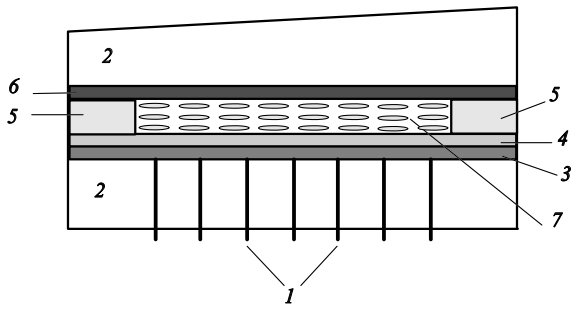

Figure 1. Scheme of the MLCC: (*1*) metal contacts; (*2*) glass substrates; (*3*) high-resistance electrode; (*4*) dielectric mirror; (*5*) spacers; (*6*) low-resistance electrode; (*7*) LC layer.

I.P.Guralnik Samara Branch, P.N.Lebedev Physics Institute, Russian Academy of Sciences, ul. Novo-Sadovaya 221, 443011 Samara, Russia; e-mail: guralnik@ssu.samara.ru;
S.A.Samagin Samara State University, ul. akad. Pavlova 1, 443011 Samara, Russia

Received 31 October 2001
Kvantovaya Elektronika **32** (4) 362–366 (2002)
Translated by M.N.Sapozhnikov

a result, the corresponding distribution of the refractive index will be produced in the LC layer, which can be controlled by varying the voltage applied to the contacts or its frequency.

In this paper, we are interested, however, in the complex resistance (impedance) of the MLCC, which is determined by currents flowing in the high-resistance and LC layers. Because the MLCC is fed with a harmonic ac voltage, the impedance between any metal contact and the low-frequency electrode is equal, by definition, to the ratio of the complex amplitudes of the voltage U_0 between these points and of the current I flowing between them. We will see below that it is more convenient to use the admittance Z^{-1} (the inverse impedance), which is related to the equivalent capacitance C and resistance R of the parallel substitution circuit by a simple expression

$$Z^{-1} = \frac{I}{U_0} = \frac{1}{R} - \mathrm{i}\omega C, \tag{1}$$

where ω is the control-signal frequency.

The current flowing through an arbitrary contact can be represented by an integral over any closed curve L encompassing this contact and lying in the plane of the control electrode [8]:

$$I = \oint_L \boldsymbol{i}\boldsymbol{N}\,\mathrm{d}l, \tag{2}$$

where $\boldsymbol{i}$ is the surface current density in the plane of the high-resistance electrode and $\boldsymbol{N}$ is the external normal to the contour L. In turn, the surface current density is expressed in terms of the electric field in the control-electrode plane, i.e., in terms of the voltage gradient as

$$\boldsymbol{i} = (-\nabla_\perp U)/\rho_\mathrm{s}, \tag{3}$$

where ρ_s is the sheet resistance of the control electrode in whose plane the differentiation is performed. Therefore, to calculate the admittance, it is necessary to know the voltage distribution over the MLCC aperture. As mentioned above, the problem of voltage distribution was considered in paper [4], where the solution was obtained for the axially symmetric problem appearing upon applying voltage at the central contact:

$$U = U_0 \frac{N_1(\mathrm{i}\chi l)J_0(\mathrm{i}\chi r) - J_1(\mathrm{i}\chi l)N_0(\mathrm{i}\chi r)}{N_1(\mathrm{i}\chi l)J_0(\mathrm{i}\chi a) - J_1(\mathrm{i}\chi l)N_0(\mathrm{i}\chi a)}. \tag{4}$$

Here, N_1 and N_0 are Neumann functions; J_1 and J_0 are Bessel functions; χ is the modal parameter whose square is $\chi^2 = \rho_\mathrm{s}(g - \mathrm{i}\omega c)$; g and c are the specific (per unity area) conductivity and capacitance of the LC layer, respectively; a is the radius of a metal contact; and l is the radius of the MLCC aperture. By introducing the specific impedance z of the LC layer, we can represent the modal impedance χ in the form

$$\chi^2 = \rho_\mathrm{s}(g - \mathrm{i}\omega c) = \frac{\rho_\mathrm{s}}{z} = -\frac{\mathrm{i}\omega\varepsilon_0\varepsilon^*\rho_\mathrm{s}}{d}, \tag{5}$$

where $\varepsilon^* = \varepsilon' + \mathrm{i}\varepsilon''$ is the complex permittivity of the LC layer; d is the layer thickness; and ε_0 is the free space permittivity.

By using relations (1)–(4), we obtain finally the expression for the MLCC admittance for the axially symmetric voltage distribution:

$$Z^{-1} = \frac{2\pi a}{\rho_\mathrm{s}}\mathrm{i}\chi\frac{N_1(\mathrm{i}\chi l)J_1(\mathrm{i}\chi a) - J_1(\mathrm{i}\chi l)N_1(\mathrm{i}\chi a)}{N_1(\mathrm{i}\chi l)J_0(\mathrm{i}\chi a) - J_1(\mathrm{i}\chi l)N_0(\mathrm{i}\chi a)} + \frac{\pi a^2}{z}. \tag{6}$$

Here, the last term takes into account the contribution of the part of the LC layer located under the metal contact to the total admittance. Note that solution (4) and, hence, expression (6) were obtained in the approximation of a constant impedance of the LC layer, when the modal parameter is assumed constant and independent of the local voltage at the LC. However, as follows from (5), in this case z and χ can depend on the applied voltage frequency.

Fig. 2 shows the frequency dependences of R and C calculated from expressions (1) and (6). We used in the calculations the real values of the MLCC geometry and of the LC physical parameters. As expected, the MLCC capacitance for the LC director aligned along the electric field was greater than that for the perpendicular orientation ($C_\parallel > C_\perp$). This is explained by the fact that the specific capacitance $c_\parallel$ is greater than $c_\perp$, which is typical for positive LCs because $\varepsilon_\parallel > \varepsilon_\perp$. The decrease of $C_\parallel$ and $C_\perp$ is caused by the localisation of the voltage distribution within a narrower region near the central contact, which reduces the effective 'area of the MLCC plates'. The effective resistance of the control electrode – LC layer system

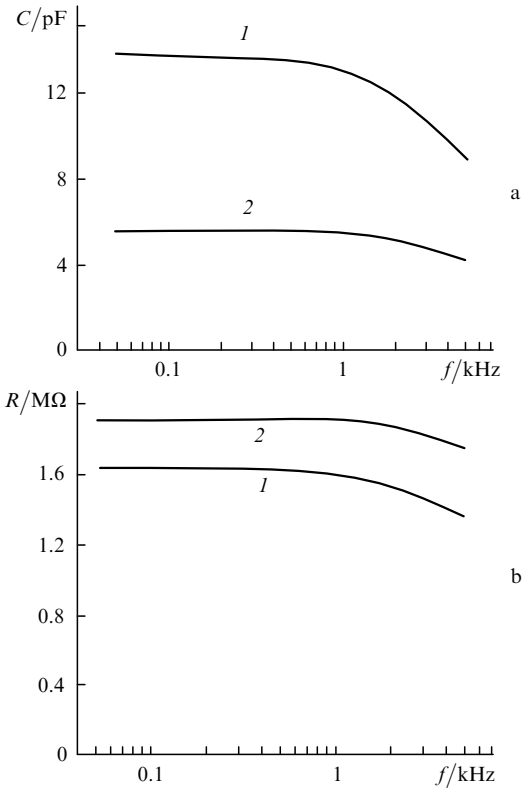

Figure 2. Frequency dependences of the equivalent capacitance (a) and resistance (b) of the corrector calculated by expressions (1), (5), and (6) for the following values of parameters: $a = 0.25$ mm, $l = 1.5$ cm, $\rho = 5$ MΩ/□. The curves were obtained by substituting to (5) $c_\parallel = 673$ pF cm^{-2}, $g_\parallel = 7.0$ (MΩ cm^2)$^{-1}$ (*1*) and $c_\perp = 177$ pF cm^{-2} and $g_\perp = 3.4$ (MΩ cm^2)$^{-1}$ (*2*).

to the applied voltage decreases for the same reason, and $R_{\parallel} < R_{\perp}$ because $g_{\parallel} > g_{\perp}$.

To compare R and C calculated from expressions (1) and (6) with experimental data, it is necessary to take into account the dependence of the LC parameters g and c in (5) and (6) on the applied voltage and its frequency. The local permittivity of nematic LCs, which are commonly used for phase modulation, can be written in the form [9]

$$\varepsilon^* = \varepsilon_{\perp}^* \cos^2\theta + \varepsilon_{\parallel}^* \sin^2\theta, \tag{7}$$

where $\varepsilon_{\perp}^*$ and $\varepsilon_{\parallel}^*$ are the principal values of the complex permittivity tensor and θ is the angle between the director and the substrate surface. Because of the delayed reorientation of LC molecules in an external electric field, the director has no time to follow a change in the instantaneous field and its orientation depends only on the average (effective) value of the field but not on its frequency. Therefore, the angle θ in (7) does not depend on the frequency of the ac control voltage, being dependent only on the effective voltage. On the contrary, permittivities in (7) do not depend on the voltage (the assumption about linear polarisation is quite justified because the control voltage lies in the range from 5 to 20 V), but depend on the frequency.

Combined measurements of the electrophysical and electrooptical parameters of various nematic LCs were performed in papers [7, 10]. However, the frequency range of these measurements had a lower limit of 500 Hz. Because, as we will see below, the MLCCs under study operates in the frequency range from 40 Hz to 5 kHz, we performed the additional study of the E-49 LC (Merck, Germany) in this frequency region. To our knowledge, this LC was not earlier studied in this respect.

3. The LC impedance

We used in the MLCC the E-49 LC. The equivalent capacitance and resistance of the LC were measured by the bridge method in a parallel substitution circuit. We used cells of different area with the initial planar orientation of the LC of area 225, 529, and 932 mm^2; the LC layer thickness was 25 μm. The sinusoidal effective voltage from 0.3 to 10.0 V in the frequency range from 40 to 30000 Hz was applied to the cell.

Fig. 3 shows a typical dependence of the LC capacitance on the applied effective voltage [the volt–farad characteristic (VFC)]. In the voltage range below the threshold voltage $U_{\rm th} = \pi[K_{11}/\varepsilon_0(\varepsilon'_{\parallel} - \varepsilon'_{\perp})]^{1/2}$ for the Fredericksz transition, the LC retains the initial planar orientation, so that the cell capacitance remains constant. For relatively high voltages $U > (5-7)U_{\rm th}$, the LC layer is almost entirely oriented along the electric field and the VFC exhibits saturation. The resistance of the LC cell exhibits the similar voltage dependence, the only difference being that the resistance below the threshold was lower than that upon saturation. Having measured capacitances and resistances at different frequencies, we calculated the corresponding permittivities ε'_{γ} and ε''_{γ} from the expressions

$$\varepsilon'_{\gamma} = \frac{dC_{\gamma}}{S\varepsilon_0}, \qquad \varepsilon''_{\gamma} = \frac{1}{2\pi\varepsilon_0}\frac{d}{SfR_{\gamma}} \quad (\gamma = \perp, \parallel). \tag{8}$$

Unlike C and R, permittivities are independent of the cell geometry and are entirely determined by the LC properties. The frequency dependences obtained in this way (Fig. 4) show that $\varepsilon'_{\perp}$ and $\varepsilon'_{\parallel}$ remain virtually invariable in the frequency range from 10^2 to 10^4 Hz and drastically increase with decreasing frequency. In addition, $\varepsilon'_{\parallel}$ begins to decrease for $f > 10$ kHz. The quantities $\varepsilon''_{\perp}$ and $\varepsilon''_{\parallel}$ are inversely proportional to the frequency, the slope of the frequency dependence of $\varepsilon''_{\parallel}$ drastically decreasing at 10 kHz.

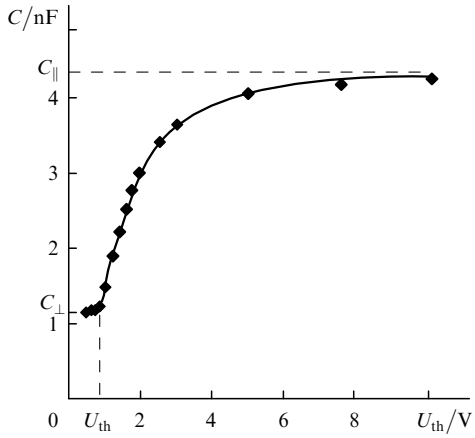

Figure 3. Volt–farad characteristic of the LC cell of area $S = 5.29$ cm^2 at the frequency $f = \omega/2\pi = 100$ Hz; $U_{\rm th}$ is the LC threshold voltage; $C_{\perp}$ and $C_{\parallel}$ are the limiting capacitances for the LC director oriented perpendicular and parallel to the external electric field, respectively.

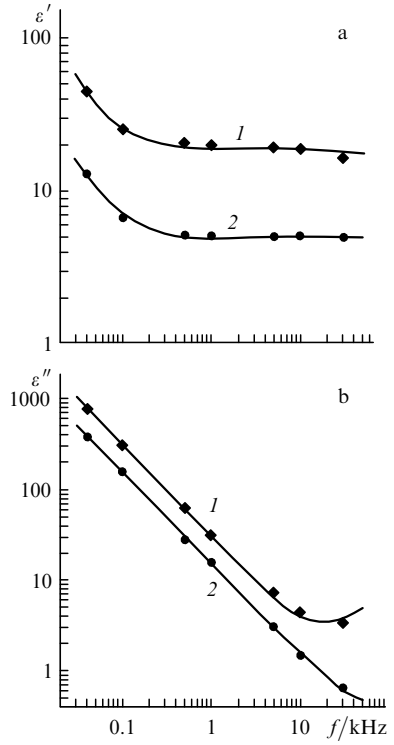

Figure 4. Dispersion of the real (a) and imaginary (b) parts of the permittivity of the E-49 LC for the LC director oriented parallel (*1*) and perpendicular (*2*) to the electric field (circles and squares are experiment; curves are calculated from (10)).

The dispersion of the permittivity in nematic LCs is commonly related to the Debye relaxation [9]. We assume that the Debye relaxation really occurs in the LC under study, which is confirmed by the presence of horizontal parts in the curves of frequency dependences of $\varepsilon'_\perp$ and $\varepsilon'_\parallel$. However, the low-frequency permittivity may also depend on the conductivity of ions, which are present in the LC. The contribution from these ions to the complex permittivity can be written in the form [11]

$$\varepsilon_{\mathrm{i}}^{*} = \frac{\sqrt{2} n q^2 D^{3/2}}{\varepsilon_0 d k_{\mathrm{B}} T \omega^{3/2}} + \mathrm{i}\frac{n q^2 D}{\varepsilon_0 k_{\mathrm{B}} T \omega}, \tag{9}$$

where n, q, and D are the concentration, charge, and diffusion coefficient of ions, respectively; T is the absolute temperature; and k_{B} is the Boltzmann constant. Although expression (9) was obtained for polymers, it adequately describes ion processes in LCs, for example, in a popular LC 5-cyanobiphenyl [12].

We interpreted our experimental data using the theoretical expression that describes both the ionic conductivity and the Debye relaxation of the LC with the characteristic time τ_{D}:

$$\varepsilon'_\gamma = \varepsilon_\gamma(\infty) + \frac{\varepsilon_\gamma(0) - \varepsilon_\gamma(\infty)}{1 + (2\pi f \tau_{\gamma\mathrm{D}})^2} + \frac{n q^2 D_\gamma^{3/2}}{2\pi\varepsilon_0\sqrt{\pi} d k_{\mathrm{B}} T} f^{-3/2},$$
$$\varepsilon''_\gamma = \frac{[\varepsilon_\gamma(0) - \varepsilon_\gamma(\infty)] 2\pi f \tau_{\mathrm{D}}}{1 + (2\pi f \tau_{\gamma\mathrm{D}})^2} + \frac{n q^2 D_\gamma}{2\pi\varepsilon_0 k_{\mathrm{B}} T} f^{-1}, \tag{10}$$

where $\varepsilon_\gamma(0)$ and $\varepsilon_\gamma(\infty)$ are the permittivities for $\omega\tau_{\gamma\mathrm{D}} \ll 1$ and $\omega\tau_{\gamma\mathrm{D}} \gg 1$, respectively. We used the method of least squares with a simultaneous optimisation of all four expressions (10) over eight parameters: $\varepsilon_\perp(0)$, $[\varepsilon_\perp(0) - \varepsilon_\perp(\infty)]2\pi\tau_\perp$, $\varepsilon_\parallel(0)$, $\varepsilon_\parallel(0) - \varepsilon_\parallel(\infty)$, $\tau_\parallel$, n, $D_\parallel$, and $D_\perp$. The results of the optimisation are shown by curves in Fig. 4 and presented in Table 1 along with data obtained in other papers. We used the LC parameters obtained in this way for simulating the electrophysical properties of the MLCC.

4. Experimental study of the MLCC

Because we obtained the quantitative expression for the MLCC impedance for the case when the voltage distribution has the axial symmetry, we studied experimentally the MLCC impedance between the central contact and the low-resistance electrode. We investigated the MLCC that was based on the E-49 LC and had 37 metal contacts forming a hexagonal structure with a side of 3.3 mm. The radius of contacts was $a = 0.25$ mm and the radius of the corrector aperture was $l = 15$ mm. The measurements were performed in the frequency range from 40 to 5000 Hz for voltages varying from 0.4 to 7.0 V.

By using the experimental voltage dependences of the corrector capacitance and resistance obtained at different frequencies (Fig. 5), we plotted the frequency characteristics of these quantities for $U = 0.5$ and 7.0 V, which are shown in Fig. 6. Fig. 6 also presents the corresponding theoretical dependences, which were derived by substituting the frequency characteristics (10) to expression (6). We used in this case the LC parameters that were measured in LC cells (columns 2–6 in Table 1) because this LC was employed in the MLCC. On the other hand, the ion parameters in a cell and the MLCC may differ because of the difference in assembling the cell and corrector. For this reason, we selected the values of n, $D_\parallel$, and $D_\perp$ during optimisation, as described in Section 3.

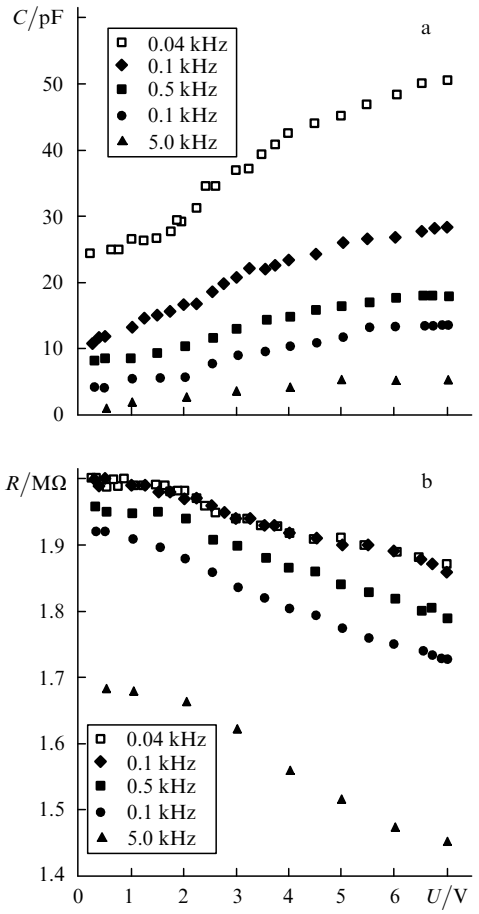

Figure 5. Voltage dependences of the MLCC capacitance (a) and resistance (b) at different frequencies.

In addition, we took into account in the calculations a wiring capacitance between wires through which the control voltage was applied to the metal contacts, which was connected in parallel and was 13.5 pF. Because the threshold LC voltage was $U_{\mathrm{th}} > 0.5$ V, curves (*1*) in Fig. 6 describe the situation when the LC molecules are not reoriented by an external electric field, i.e., $\varepsilon = \varepsilon_\perp$ at all points of the aperture. In this sense, the curves in Fig. 6 are

Table 1. The LC parameters obtained by approximation and their comparison with data obtained in other papers.

References	$\varepsilon_\perp(0)$	$\varepsilon_\parallel(0)$	$[\varepsilon_\perp(0) - \varepsilon_\perp(\infty)]2\pi\tau_\perp$/s	$\varepsilon_\parallel(\infty)$	$\tau_\parallel$/s	n/cm^{-3}	$D_\perp$/cm^2 s^{-1}	$D_\parallel$/cm^2 s^{-1}
This paper	4.99	18.97	3.37×10^{-6}	3.06	0.9×10^{-6}	2.67×10^{13}	6.4×10^{-7}	9.1×10^{-7}
E-49 passport	5.1	21.7	–	–	–	–	–	–
Typical values [9]	–	–	–	–	$\sim 10^{-6}$	–	–	–
For 5CB [12]	–	–	–	–	–	2×10^{14}	4×10^{-8}	–

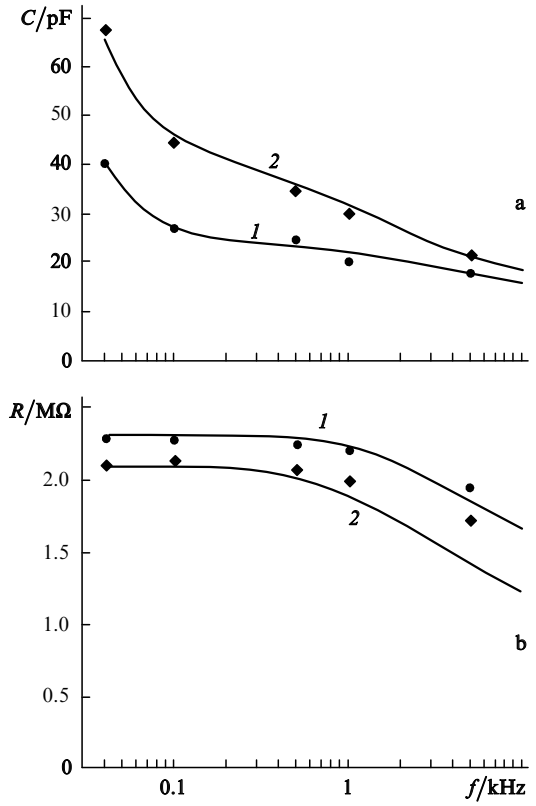

Figure 6. Calculated (curves) and experimental (circles and squares) frequency dependences of the equivalent capacitance (a) and resistance (b) of the corrector for voltages 0.5 (*1*) and 7 V (*2*) and $n = 1.79 \times 10^{14}$ cm^{-3}, $D_{\perp} = 2.8 \times 10^{-6}$ cm^2 s^{-1}, and $D_{\parallel} = 4.9 \times 10^{-6}$ cm^2 s^{-1}.

similar to the corresponding curves in Fig. 2. The situation for $U = 7.0$ V is more complicated because $U(r) > U_{\text{th}}$ only within some region near the central contact due to a decrease in the voltage with distance from the central contact. Therefore, the approximation $\varepsilon = \varepsilon_{\parallel}$ is not valid for the entire MLCC aperture.

However, because we estimated the impedance by calculating the current as an integral over the circle adjacent to the contact, the results of the calculation (curves *2* in Fig. 6) are in good agreement with the experiment. Curves *1* in Fig. 6 also well agree with the experiment. A comparison of Fig. 6 with Figs 2 and 4 shows that for frequencies below 1 kHz the MLCC parameters substantially depend on the ionic conductivity, whereas at higher frequencies these parameters depend on the localisation of the voltage distribution near the central contact, which reduces both the capacitance and resistance with increasing frequency.

We calculated the MLCC quality ωRC from the data presented in Fig. 5. The MLCC quality factor does not exceed 0.24 for all the parameters of the control voltage, i.e., the MLCC represents an active load for a control signal generator.

5. Conclusions

We have calculated and experimentally studied for the first time the impedance of a modal multichannel LC wavefront corrector. The separate study of the LC used in the corrector showed that its permittivity at frequencies up to several kilohertz is determined by the ionic conductivity and Debye relaxation. These factors also determine the MLCC impedance in the frequency region up to 1 kHz. However, at higher frequencies, the localisation of the voltage near the contact comes into play along with these factors. The influence of ions on the electric parameters of the LC is undesirable. It can be eliminated by using higher frequencies to control the MLCC if the resistance of the control electrode is reduced, which is quite realistic from the technological point of view. The calculated capacitance and resistance of the LC cell and MLCC are in good agreement with their experimental values.

Acknowledgements. The authors thank A.F.Naumov and M.Yu.Loktev for useful discussions and valuable comments. This work was partially supported by the INTAS-ESA (Grant No. 99-0523) and the Integration Program (Contract No. 235).

References

1. Naumov A.F., Loktev M.Yu., Guralnik I.R., Vdovin G.V. *Opt. Lett.*, **23**, 992 (1998).
2. Zayakin O.A., Loktev M.Yu., Love G.D., Naumov A.F. *Proc. SPIE Int. Soc.Opt. Eng.*, **3983**, 112 (1999).
3. Guralnik I.R., Loktev M.Yu., Love G.D., Naumov A.F. *Proc. SPIE Int. Soc.Opt. Eng.*, **4338**, 171 (2000).
4. Naumov A.F., Vdovin G.V. *Opt. Lett.*, **23**, 1550 (1998).
5. Kotova S.P., Guralnik I.R., Klimov N.A., Kvashnin M.Yu., Loktev M.Yu., Love G.D., Naumov A.F., Rakhmatulin M.A., Vdovin G.V., Zayakin O.A. *Rep. X Intern. Conf. «Laser Optics 2000»* (St. Petersburg, Russia, 2000).
6. Hirabayashi K. *Opt. Lett.*, **21**, 1484 (1996).
7. Guralnik I.R., Belopukhov V.N., Love G.D., Naumov A.F. *J. Appl. Phys.*, **87**, 4069 (2000).
8. Vdovin G.V., Guralnik I.R., Kotova S.P., Loktev M.Yu., Naumov A.F. *Kvantovaya Elektron.*, **26**, 256 (1999) [*Quantum. Electron.*, **29**, 256 (1999)].
9. Blinov L.M. *Elektro- i magnitooptika zhidkikh kristallov* (Electro- and Magnetooptics of Liquid Crystals) (Moscow: Nauka, 1978).
10. Guralnik I.R., Naumov A.F., Belopukhov V.N. *Proc. SPIE Int. Soc.Opt. Eng.,* **3684**, 28 (1998).
11. Uemura S. *J. Polym. Sci. A2*, **70**, R3434 (1991).
12. Naito H., Yokoyama Y., Murakami S., Imai M., Okuda M., Sugimura A. *Mol. Cryst. Liq. Cryst.*, **262**, 249 (1995)